Available online at www.sciencedirect.com
ScienceDirect
Carbohydrate Polymers 72 (2008) 369–375
Carbohydrate Polymers
www.elsevier.com/locate/carbpol

Properties of biodegradable thermoplastic pea starch/carboxymethyl cellulose and pea starch/microcrystalline cellulose composites

Xiaofei Ma [a], Peter R. Chang [b,*], Jiugao Yu [a]

[a] School of Science, Tianjin University, Tianjin 300072, China
[b] Bioproducts and Bioprocesses National Science Program, Agriculture and Agri-Food Canada, 107 Science Place, Saskatoon, SK, Canada S7N 0X2

Received 5 July 2007; received in revised form 14 August 2007; accepted 4 September 2007
Available online 11 September 2007

Abstract

Glycerol-plasticized thermoplastic pea starch (TPS)/carboxymethyl cellulose (CMC) and TPS/microcrystalline cellulose (MC) composites were respectively prepared by a screw extruder. As the reinforcement filler, the effects of CMC and MC contents on the morphology, thermal stability, dynamic mechanical thermal analysis (DMTA), mechanical properties, as well as water vapor permeability (WVP) were investigated. Scanning electron microscope (SEM) showed that there was good adhesion between starch and CMC or MC, but these superfluous cellulose derivatives resulted in the conglomeration in TPS matrix. MC increased the thermal stability, while CMC impaired it. DMTA revealed that the addition of CMC or MC enhanced the storage modulus and the glass transition temperature of the composites. At the low contents of cellulose derivatives (<9 wt%), the greater CMC or MC content were, the more the tensile strength of the composite. The values of WVP decreased with the increasing of cellulose derivatives. TPS/MC composites had better water vapor barrier than TPS/CMC composites.

Keywords: Pea starch; Carboxymethyl cellulose sodium; Microcrystalline cellulose; Composites

1. Introduction

The improper disposition of the enormous volume of petroleum-derived plastics in the environment has led to environment pollution and raised much interest in edible and biodegradable films from nature polymers, the biodegradable and renewable resources. Starch is one of the most studied and promising raw materials for the production of biodegradable plastics, which is a natural renewable carbohydrate polymer obtained from a great variety of crops. Starch is a low cost material in comparison to most synthetic plastics and is readily available. Starch has been investigated widely for the potential manufacture of products such as water-soluble pouches for detergents and insecticides, flushable liners and bags, and medical delivery systems and devices (Fishman, Coffin, & Konstance, 2000). Native starch commonly exists in a granular structure, which can be processed into thermoplastic starch (TPS) under the action of high temperature and shear by melt extrusion (Forssell, Mikkilä, & Moates, 1997; Ma & Yu, 2004).

Unfortunately, the properties of TPS are not satisfactory for some applications such as packaging materials. One approach is the use of fibers as reinforcement for TPS. The fibers described in the literature for this intention are cellulose nanocrystalites (Lu, Weng, & Cao, 2006), natural fibers (Alvarez, Vázquez, & Bernal, 2005; Soykeabkaew, Supaphol, & Rujiravanit 2004) and commercial regenerated cellulose fibers (Funke, Bergthaller, & Lindhauer, 1998). When natural fibers are mixed TPS, their mechanical properties are obviously improved, because the chemical similarities of starch and plant fibers provide a good interaction (Avérous, Fringant, & Moro, 2001; Lu et al., 2006). A significant improvement in water resistance is obtained by adding cellulose crystallites (Lu,

* Corresponding author. Tel.: +1 306 956 7637; fax: +1 306 956 7247.
E-mail address: changp@agr.gc.ca (P.R. Chang).

0144-8617/$ - see front matter
doi:10.1016/j.carbpol.2007.09.002

Weng, & Cao, 2005) or micro-fiber (Dufresne, Dupeyre, & Vignon, 2000; Ma, Yu, & Kennedy, 2005). This behavior is related to the highly crystalline 'hydrophobic' character of the cellulose fibers in comparison to starch hydrophilic property. In addition, these authors (Curvelo, de Carvalho, & Agnelli, 2001) demonstrated an improved thermal stability due to a higher and longer thermal resistance of cellulose fibers.

Pea starch is mainly available as a by-product of protein extraction. Therefore, it is considered to be a relatively cheap source of starch compared to corn, wheat and potato starches (Ratnayake, Hoover, & Warkentin, 2002). Carboxymethyl cellulose sodium (CMC) and microcrystalline cellulose (MC) have no harmful effects on human health, and are used as highly effective additive to improve the product and processing properties in various fields of application, from foodstuffs, cosmetics and pharmaceuticals to products for the paper and textile industries. In this paper, CMC and MC were used as the reinforcement filler of glycerol-plasticized thermoplastic pea starch (TPS) matrix. This work focused on processing and characterization of TPS/CMC and TPS/MC composites in terms of the morphology, thermal stability, dynamic mechanical thermal analysis, and water vapor permeability as well as the effect of water contents on mechanical properties. These polysaccharide (thermoplastic starch/cellulose derivatives) composites have the potential to replace conventional packaging such as edible films, food packaging and biodegradable packaging.

2. Experimental

2.1. Materials

Pea starch composed of 35% amylose and 65% amylopectin, and with average particle size of about 30 μm, was supplied by Nutri-Pea Limited Canada (Portage la Prairie, Canada). Granular powders of carboxymethyl cellulose sodium (CMC) and microcrystalline cellulose (MC) with the particle size of 10–50 μm were obtained from Tianjin Fine Chemical Institute. Glycerol, the plasticizer was purchased from Tianjin Chemical Reagent Factory (Tianjin, China).

2.2. The preparation of TPS/CMC and TPS/MC composites

Glycerol was blended (3000 rpm, 2 min) with pea starch and CMC (or MC) by use of a High Speed Mixer GH-100Y (made in China), and then stored overnight. The ratio of glycerol and pea starch (wt/wt) was 30:100. The mixtures were manually fed into a single screw Plastic Extruder SJ-25(s) (Screw Ratio $L/D = 25{:}1$, made in China) operating at 20 rpm. The temperature profile along the extruder barrel was based on four heating zones, which are 130, 140, 140 and 120 °C from feed zone to die. The die has a hole of 3 mm in diameter. Samples were pressed with the flat sulfuration machine into the sheet for testing.

2.3. Scanning electron microscope (SEM)

The fracture surfaces of extruded composite strips were examined using Scanning Electron Microscope Philips XL-3, operating at an acceleration voltage of 20 kV. Composite strips were cooled in liquid nitrogen, and then broken. The fracture faces were vacuum coated with gold for SEM.

2.4. Thermogravimetric analysis (TGA)

The composites for TGA were stored in tightly sealed plastic bags for one week. The thermal properties of the composites were measured with a ZTY-ZP type thermal analyzer. The sample weight varied from 10 to 15 mg. Samples were heated from room temperature to 500 °C at a heating rate of 15 °C/min.

2.5. Dynamic mechanical thermal analysis (DMTA)

The composites for DMTA were stored at 33% relative humidity (RH) for one week. The DMTA using a Mark Netzsch DMA242 analyzer was performed on the thick specimens ($40 \times 7 \times 2$ mm), in a single cantilever-bending mode at a frequency of 3.33 Hz and a strain × 2N, corresponding to the maximum displacement amplitude of 30 μm. The range of temperature was from −100 to 100 °C. The standard heating rate used was 3.0 °C/min.

2.6. Mechanical testing

Composites were pressed with the flat sulfuration machine into the sheet. The Testometric AX M350-10KN Materials Testing Machine was operated at a crosshead speed of 50 mm/min for tensile testing (ISO 1184–1983 standard). The data was averaged over 5–8 specimens.

In order to analyze the effect of environmental humidity on mechanical properties of the composites, the composites were stored in closed chambers over several aqueous mixtures at 25 °C for a period of time. The materials used were dried silica gel, $MgCl_2$ saturated solution and NaCl saturated solution, providing RH of 0%, 33% and 75%, respectively.

The original water content (dry basis) of composites was determined gravimetrically by drying small pieces of TPS at 105 °C overnight, and the evaporation of glycerol was negligible (Curvelo et al., 2001). When composites were stored for a period of time at RH of 0% or 75%, water content (C) was calculated on the base of the original weight (W_0), the current weight (W) and the original water content (C_0).

$$C = \frac{W - W_0(1 - C_0)}{W(1 - C_0)} \times 100\% \quad (1)$$

2.7. Water vapor permeability (WVP)

WVP tests were carried out by ASTM method E96 (1996) with some modifications (Mali, Grossmann, Garcıa, Martino, & Zaritzky, 2006). The films (about 0.5 mm thickness) were cut into circle shapes, sealed over with melted paraffin, and stored in a desiccator at 25 °C. RH 0% was maintained with anhydrous calcium chloride in the cell. Each cell was placed in a desiccator containing saturated sodium chloride to provide a constant RH 75%. Water vapor transport was determined by the weight gain of the permeation cell. Changes in the weight of the cell were recorded as a function of time. Slopes were calculated by linear regression (weight changes vs. time) and the correlation coefficient for all reported data was >0.99. The water vapor transmission rate (WVTR) was defined as the slope (g/s) divided by the transfer area (m^2). After the permeation tests, film thickness was measured and WVP ($g\ Pa^{-1}\ s^{-1}\ m^{-1}$) was calculated as

$$\mathrm{WVP} = \frac{\mathrm{WVTR}}{P(R_1 - R_2)} \cdot x \tag{2}$$

where P is the saturation vapor pressure of water (Pa) at the test temperature (25 °C); R_1, the RH in the desiccator; R_2, the RH in the permeation cell and x is the film thickness (m). Under these conditions, the driving force $[P(R_1 - R_2)]$ is 1753.55 Pa.

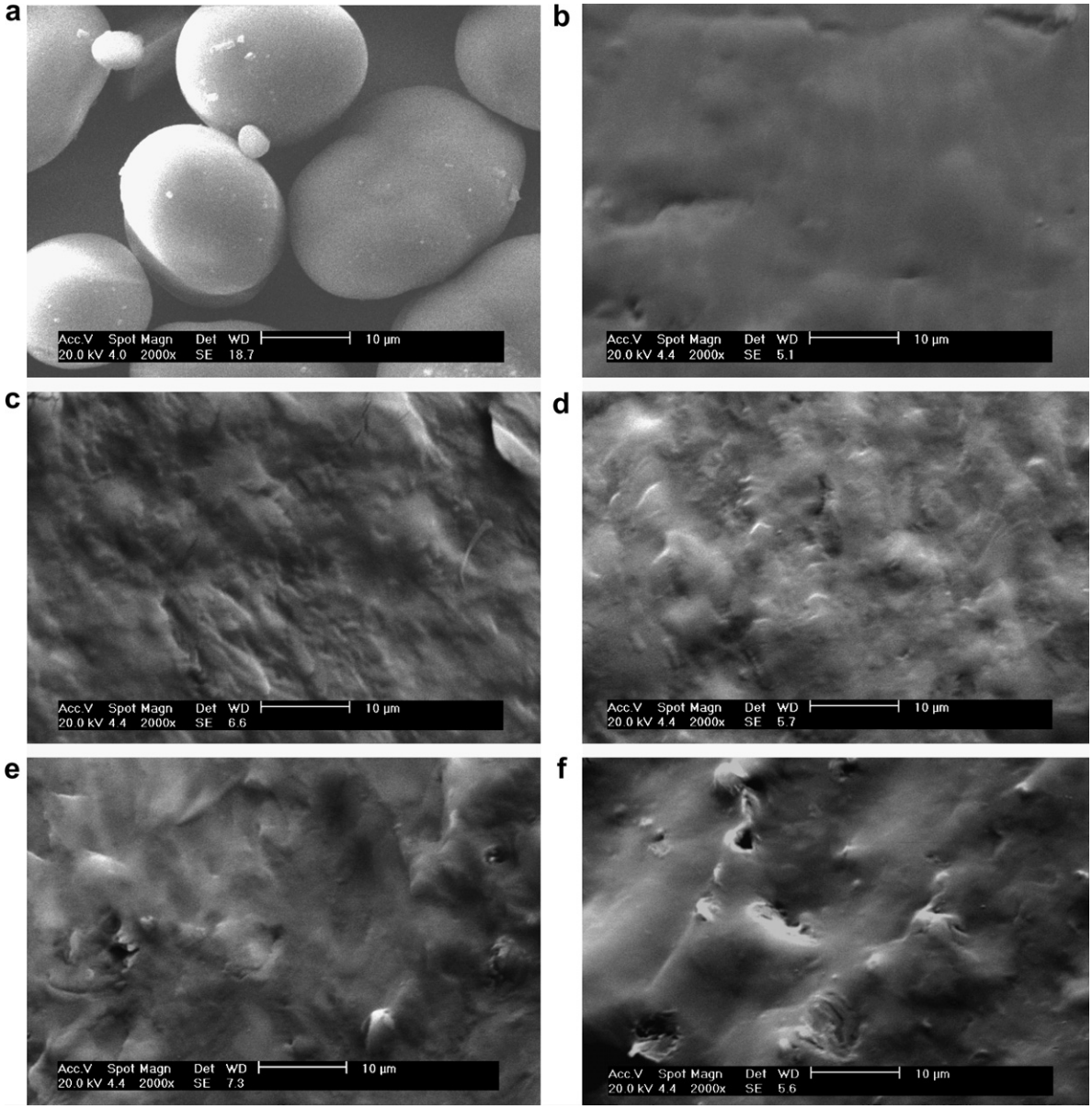

Fig. 1. SEM micrograph at 2000× magnification for native pea starch and the fragile fractured surface of TPS filled with different CMC and MC contents. (a) Native pea starch, (b) TPS, (c) TPS/CMC composites (6 wt% CMC), (d) TPS/CMC composites (12 wt% CMC), (e) TPS/MC composites (6 wt% MC), (f) TPS/MC composites (12 wt% MC).

3. Results and discussion

3.1. Microscopy

The morphology structure of polymer composites is a very important characteristic because it ultimately determines many properties of the polymer composites. An SEM micrograph at 2000× magnification of native starch granules and the fractured surface of TPS filled with different CMC and MC contents are shown in Fig. 1. Compared with native pea starch granules (Fig. 1(a)), no residual granular structure was present in the continuous TPS phase. Because of the high shear and temperature conditions with the action of glycerol, native pea starch granules were molten or physically broken up into small fragments. Plasticizers are known to disrupt intermolecular and intramolecular hydrogen bonds and make the native starch plastic (Ma, Yu, & Wan, 2006).

The introduction of CMC and MC had no effect on the plasticization of pea starch, because there was no residual starch granular structure, as shown in Fig. 1(c–f). The surface of cellulose derivatives appeared to be covered by TPS, which was attributed to strong interaction between the cellulose derivatives and TPS due to their chemical similarities. The conglomeration of CMC and MC appeared at high filler content (12 wt%), and was more obvious for TPS/MC composites than TPS/CMC composites.

3.2. TGA

Thermogravimetric analysis (TGA) was performed for the composites, where the mass loss due to the volatilization of the degradation products was monitored as a function of temperature. The thermogravimetric (TG) and Derivative thermogravimetric (DTG) curves of TPS, TPS/CMC and TPS/MC composites in air at a heating rate of 15 °C/min are shown in Figs. 2 and 3, respectively. In

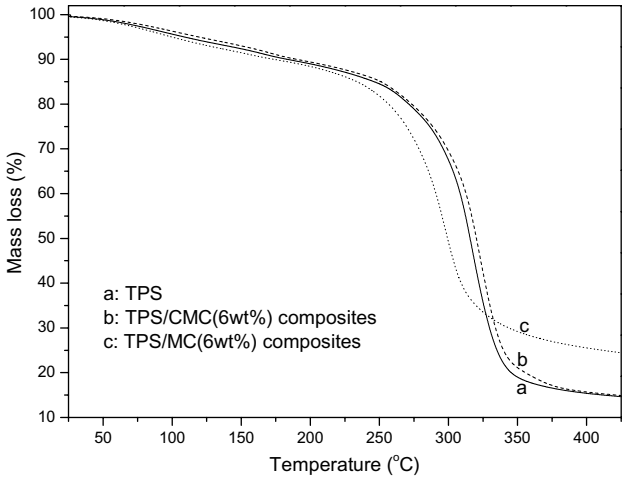

Fig. 2. Thermogravimetric curves for TPS, TPS/CMC and TPS/MC composites at a heating rate of 15 °C/min in air.

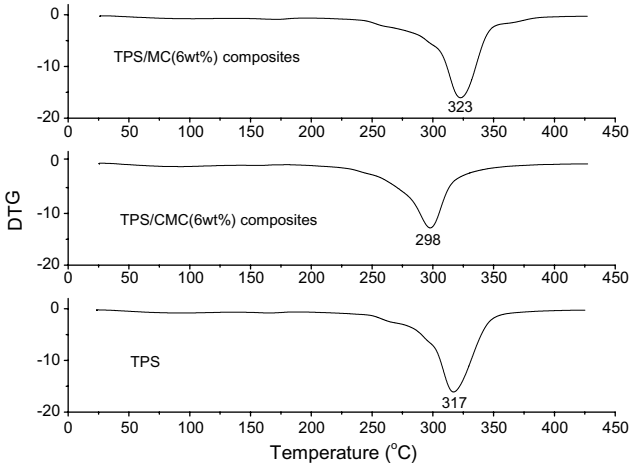

Fig. 3. Derivative thermogravimetric curves for TPS, TPS/CMC and TPS/MC composites at a heating rate of 15 °C/min in air.

Fig. 2, the mass loss below 100 °C was mainly ascribed to water loss. The mass loss before the onset temperature was related to the volatilization of both water and glycerol (Ma, Yu, & Ma, 2005). The tiny differences of mass loss among TPS, TPS/CMC and TPS/MC composites at onset temperature, were mainly due to the similar contents of water and glycerol. The decomposed temperature, T_{max} was the temperature at maximum rate of mass loss, i.e. the peak temperature shown in Fig. 3. The degradation of TPS, TPS/CMC and TPS/MC composites took place at 317, 298 and 323 °C, respectively. The addition of CMC resulted in the decrease of thermal stability, which was ascribed to the poor thermal stability of CMC. However, the introduction of MC increased thermal stability, which was related to the good thermal stability of crystalline structure for MC and the good interaction between MC and TPS.

3.3. DMTA

DMTA is a very useful technique to study the viscoelastic response of the polymers as well as their composites in a wide range of temperatures. The behavior of storage modulus for TPS with different CMC or MC contents is shown in Fig. 4. The storage modulus for TPS/CMC or TPS/MC composites was higher than that for pure TPS. It is known that storage modulus detected by DMTA are related to the stiffness. The stiffness of composites increased with the increasing of CMC or MC contents. This improvement was possibly associated with the interaction between TPS and CMC (or MC).

In general, the storage modulus decreased as the temperature increased. However, in the region corresponding to the maximum in loss factor (tan delta) plots, the decrease of storage modulus was unusually rapid. Fig. 5 showed the curves of loss factor (tan delta) as a function of temperature for TPS/CMC or TPS/MC composites. The loss factor was sensitive to the molecular motions and its peak was

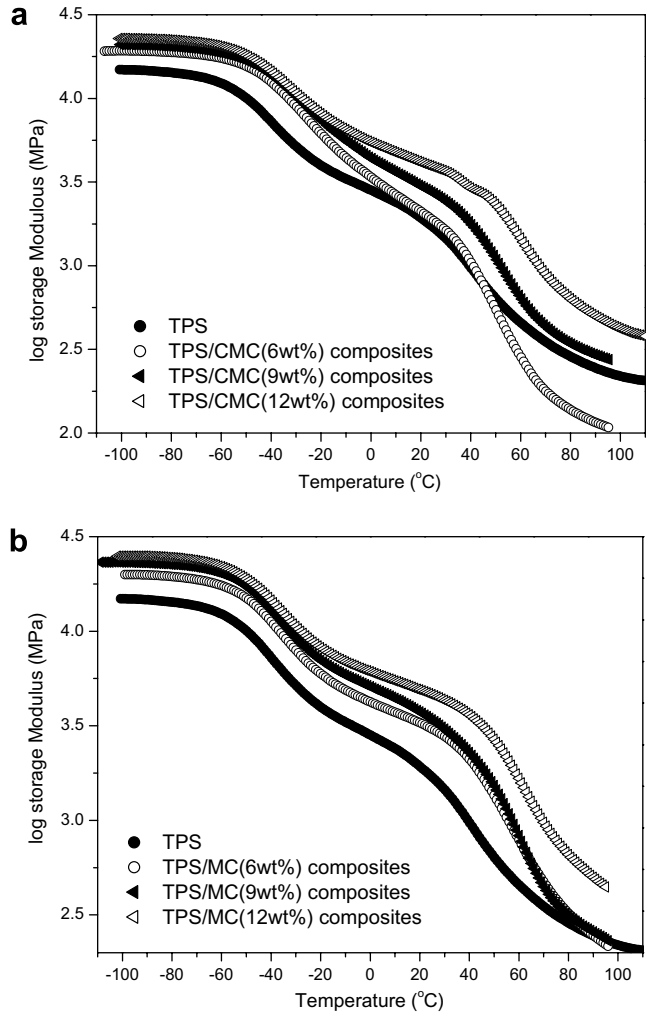

Fig. 4. DMTA (storage modulus) of TPS/CMC (a) and TPS/MC (b) composites.

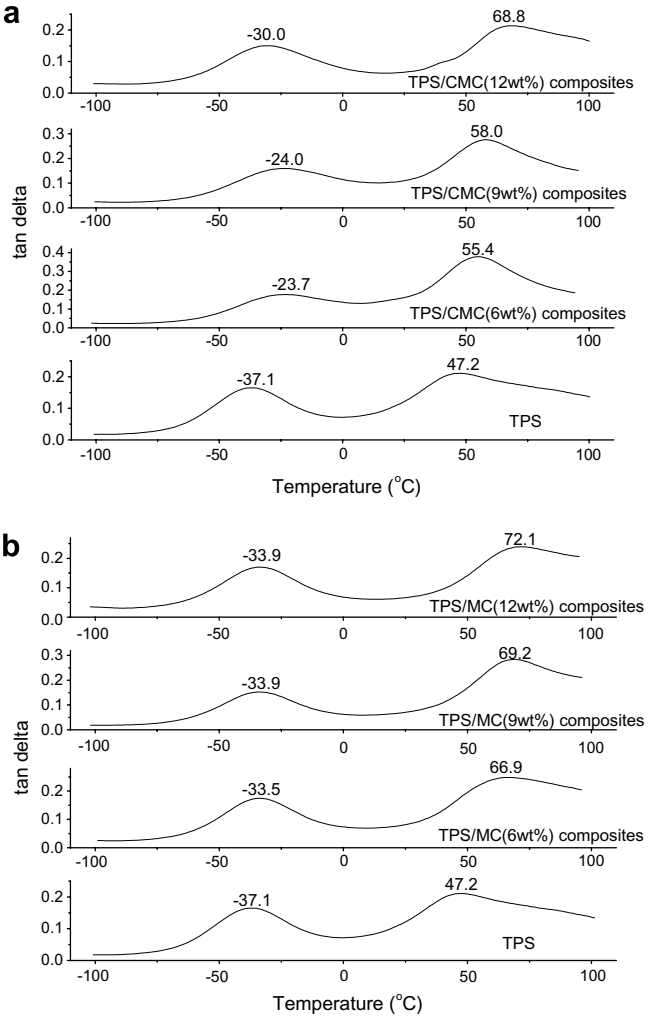

Fig. 5. DMTA (tan delta) of TPS/CMC (a) and TPS/MC (b) composites.

related to the glass transition temperature. The curve of TPS revealed two thermal transitions. There are several different viewpoints for two thermal transitions of TPS. Here an explanation was favored in terms of the transitions corresponding to two separate phases in TPS. The upper transition (47.2 °C) was clearly due to a starch-rich phase, which was regarded as the glass transition temperature (T_g) of TPS materials, whereas the lower transition (−37.1 °C) was due to a starch-poor phase (Forssell et al., 1997).

In TPS/CMC (or TPS/MC) composites, both starch-rich phase and starch-poor phase could form composites with CMC (or MC), respectively, which indicates that both the upper transition and the lower transition shifted to higher temperature. However, the effect of CMC (or MC) contents on the upper transition was more obvious and erratic than on the lower transition. The upper transition of the composites became higher with the increasing content of cellulose derivatives. As the physical joint, CMC (or MC) improved the intermolecular interaction of TPS in the starch-rich phase, which brought adjacent starch chains closer, reduced the free volume and raised the glass transitions of composites.

3.4. Mechanical properties

Water sensitivity is another important criterion for many practical applications of starch products. TPS with different CMC or MC contents were conditioned at different RHs (0% and 75%). Changes in the environmental humidity and storage time greatly affected the water contents of TPS, which, in turn induced large changes in mechanical properties. As shown in Figs. 6 and 7, the effect of the different CMC or MC contents on mechanical properties of TPS varied with increasing water contents similarly. That is, the elongation of all samples decreased when the water contents deviated from a certain value (about 10%), while the materials gradually lost tensile strength with the increase of water contents.

In the situation of low water contents (<13%) and low CMC or MC contents (<9%), the greater CMC or MC content were, the greater the tensile strength of TPS. The increase of tensile strength indicates that TPS was suited

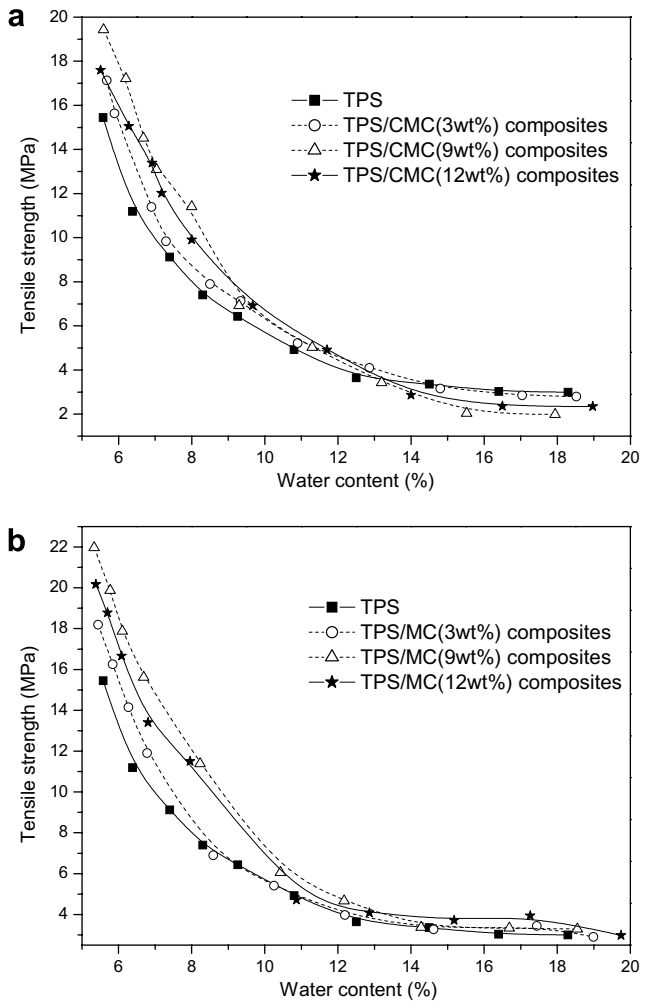

Fig. 6. The effect of cellulose and water contents on tensile stress of TPS/CMC (a) and TPS/MC (b) composites.

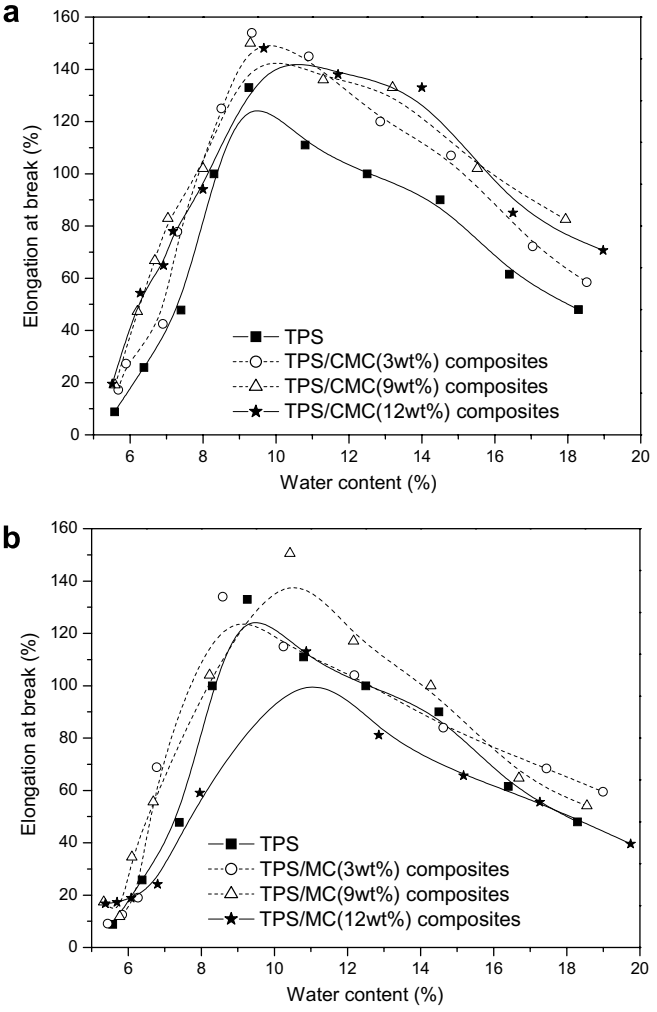

Fig. 7. The effect of cellulose and water contents on elongation at break of TPS/CMC (a) and TPS/MC (b) composites.

as the matrix for cellulose derivative (CMC or MC) filler. This was due to the remarkable intrinsic adhesion of the filler–matrix interface caused by the chemical similarity (polysaccharide structure) of starch and cellulose derivatives. The existence of such interaction, related to the contents of the filler, has already been confirmed by Avérous et al. (2001). The reinforcement effect increased with the contents of cellulose derivatives at the same water contents. However, the redundant CMC or MC (12% content) could induce the conglomeration, as indicated by SEM, which actually decreased the effective contents of filler. Thus, TPS with 12% CMC or MC contents exhibited lower tensile strength than that with 9% CMC or MC contents, as shown in Fig. 6.

With the increase of water contents, this reinforcement effect was gradually weakened, because water could separately form the interaction with starch and cellulose derivatives, and then substitute original interaction between starch and cellulose derivatives. At the high water contents (>13%), the filler contents would have few effects on the tensile strength, and CMC or MC could also soften, owing to water absorption.

When CMC or MC was added, TPS basically had an increasing elongation at break, over the whole range of water contents. But there was an exception, i.e. TPS

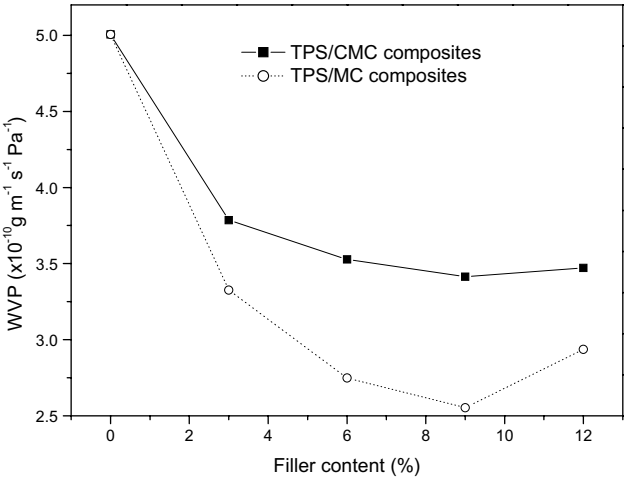

Fig. 8. The effect of CMC and MC contents on water vapor permeability of the composites.

containing the redundant CMC or MC (12% content) had a lower elongation at break than that with CMC or MC (9% content). This exception could also be related to the conglomeration of redundant CMC or MC.

3.5. Water vapor permeability

As a food packaging, film is often required to avoid or at least to decrease moisture transfer between the food and the surrounding atmosphere, and water vapor permeability should be as low as possible. As shown in Fig. 8, water vapor permeability in TPS/CMC and TPS/MC composites showed the same trend with the increasing of filler contents. Water vapor easily permeated TPS film with the highest WVP value at 5.01 g m^{-1} s^{-1} Pa^{-1}. When 3 wt% filler was added into TPS, WVP values obviously decreased. With the increase of filler contents, WVP values decreased gradually. At a content of 9 wt% filler, both TPS/CMC and TPS/MC composites showed the lowest WVP values at 3.41 and 2.55 g m^{-1} s^{-1} Pa^{-1}, respectively. When the filler content was more than 9 wt%, WVP values increased.

Water resistance of CMC and MC was better than TPS matrix. The addition of CMC and MC probably introduced a tortuous path for water molecule to pass through (Kristo & Biliaderis, 2007). At a low content of filler, CMC and MC dispersed well in the TPS matrix (as shown by SEM), and blocked the water vapor. However, superfluous filler was easy to congregate (as shown by SEM), which actually decreased the effective contents of filler and facilitated the water vapor permeation. At the same content of filler, TPS/MC composites had better water vapor barrier than TPS/CMC composites because the hydrophobic crystalline of MC led to the reduction of permeability.

4. Conclusions

In this paper, the biodegradable polysaccharide (thermoplastic starch/cellulose derivatives) composites were prepared as potential edible films, food packaging and biodegradable packaging, etc. The introduction of CMC and MC improved the storage modulus and the glass transition temperature of the composites. MC increased the thermal stability, while CMC decreased the thermal stability. Both CMC and MC increased the tensile stress and elongation at break at the low water content (13%), as well as the barrier of water vapor. This was ascribed to the good interaction between cellulose derivatives and starch. However, superfluous cellulose derivatives resulted in the conglomeration in TPS matrix, which actually decreased their effective contents. TPS/MC composites have better water vapor barrier than TPS/CMC composites because of the hydrophobic crystalline of MC.

References

Alvarez, V., Vázquez, A., & Bernal, C. (2005). Fracture behavior of sisal fiber-reinforced starch-based composites. *Polymer Composites, 26*, 316–323.

Avérous, L., Fringant, C., & Moro, L. (2001). Plasticized starch–cellulose interactions in polysaccharide composites. *Polymer, 42*, 6565–6572.

Curvelo, A. A. S., de Carvalho, A. J. F., & Agnelli, J. A. M. (2001). Thermoplastic starch-cellulosic fibers composites: Preliminary results. *Carbohydrate Polymer, 45*, 183–188.

Dufresne, A., Dupeyre, D., & Vignon, M. R. (2000). Cellulose microfibrils from potato tuber cells: Processing and characterization of starch-cellulose microfibril composites. *Journal of Applied Polymer Science, 76*, 2080–2092.

Fishman, M. L., Coffin, D. R., & Konstance, R. P. (2000). Extrusion of pectin/starch blends plasticized with glycerol. *Carbohydrate Polymers, 41*, 317–325.

Forssell, P. M., Mikkilä, J. M., & Moates, G. K. (1997). Phase and glass transition behaviour of concentrated barley starch–glycerol–water mixtures, a model for thermoplastic starch. *Carbohydrate Polymers, 34*, 275–282.

Funke, U., Bergthaller, W., & Lindhauer, M. G. (1998). Processing and characterization of biodegradable products based on starch. *Polymer Degradation and Stability, 59*, 293–296.

Kristo, E., & Biliaderis, C. G. (2007). Physical properties of starch nanocrystal-reinforced pullulan films. *Carbohydrate Polymers, 68*, 146–158.

Lu, Y. S., Weng, L. H., & Cao, X. D. (2005). Biocomposites of plasticized starch reinforced with cellulose crystallites from cottonseed linter. *Macromolecular Bioscience, 5*, 1101–1107.

Lu, Y. S., Weng, L. H., & Cao, X. D. (2006). Morphological, thermal and mechanical properties of ramie crystallites-reinforced plasticized starch biocomposites. *Carbohydrate Polymers, 63*, 198–204.

Ma, X. F., & Yu, J. G. (2004). The plasticizers containing amide groups for thermoplastic starch. *Carbohydrate Polymers, 57*, 197–203.

Ma, X. F., Yu, J. G., & Kennedy, J. F. (2005). Studies on the properties of natural fibers-reinforced thermoplastic starch composites. *Carbohydrate Polymers, 62*, 19–24.

Ma, X. F., Yu, J. G., & Ma, Y. B. (2005). Urea and formamide as a mixed plasticizer for thermoplastic wheat flour. *Carbohydrate Polymers, 60*, 111–116.

Ma, X. F., Yu, J. G., & Wan, J. J. (2006). Urea and ethanolamine as a mixed plasticizer for thermoplastic starch. *Carbohydrate Polymers, 64*, 267–273.

Mali, S., Grossmann, M. V. E., Garcıa, M. A., Martino, M. N., & Zaritzky, N. E. (2006). Effects of controlled storage on thermal, mechanical and barrier properties of plasticized films from different starch sources. *Journal of Food Engineering, 75*, 453–460.

Ratnayake, W. S., Hoover, R., & Warkentin, T. (2002). Pea starch: Composition, structure and properties – A review. *Starch/Stärke, 54*, 217–234.

Soykeabkaew, N., Supaphol, P., & Rujiravanit, R. (2004). Preparation and characterization of jute- and flax-reinforced starch-based composite foams. *Carbohydrate Polymer, 58*, 53–63.